Symmetry and spectral statistics of the magnetic band structure of a one-dimensional surface superlattice

2001 J. Phys.: Condens. Matter 13 9505

(http://iopscience.iop.org/0953-8984/13/42/311)

INSTITUTE OF PHYSICS PUBLISHING JOURNAL OF PHYSICS: CONDENSED MATTER

J. Phys.: Condens. Matter **13** (2001) 9505–9514 PII: S0953-8984(01)24003-X

Symmetry and spectral statistics of the magnetic band structure of a one-dimensional surface superlattice

H Q Xu[1,2,4] **and Ben-Yuan Gu**[3]

[1] Solid State Physics, Lund University, PO Box 118, SE-221 00 Lund, Sweden
[2] Physics Department, Dalian University of Technology, Dalian 116023, China
[3] Institute of Physics, Chinese Academy of Sciences, PO Box 603, Beijing 100080, China

E-mail: hongqi.xu@ftf.lth.se (H Q Xu)

Received 18 April 2001, in final form 21 June 2001
Published 5 October 2001
Online at stacks.iop.org/JPhysCM/13/9505

Abstract

We report a theoretical study of the spectral statistics of a quasi-one-dimensional surface superlattice in perpendicularly applied magnetic fields. The energy-level-spacing distribution and the Dyson–Mehta Δ_3 statistic of the magnetic band structure of the system are calculated. The calculations show that for the system with inversion symmetry, the magnetic band structure at the wave vector $k = 0$ is well described by the statistic derived by a superposition of two independent Gaussian orthogonal ensemble (GOE) statistics. This result is consistent with the fact that the system shows a false time-reversal violation and a real-space symmetry. The calculations show also that when the wave vector k is moved away from the $k = 0$ point, the statistical properties of the magnetic band structure are excellently described by the GOE statistics. The GOE statistics are also found in the magnetic band structure when the inversion symmetry is removed from the system.

1. Introduction

The recently developed field of physics named quantum chaos [1] has its origin in studies of spectral statistics of quantum systems whose corresponding classical dynamics exhibits chaos. The idea and methods of quantum chaos are quite general and can be applied to a broad range of quantum systems including, e.g., atoms [2–4], nuclei [5, 6], electron billiards [7, 8], as well as classical wave-mechanical systems such as vibrating plates [9, 10] and microwave cavities [11, 12].

Recently, spectral statistics has been used in the description of electronic band structures of periodic systems [13–17]. It has been shown [14] that around the centre of mass (CM) of an irreducible part of the Brillouin zone (BZ) the band structure of Si crystal shows the

[4] Author to whom any correspondence should be addressed.

Gaussian orthogonal ensemble (GOE) statistics, while the band structure of $Al_xGa_{1-x}As$ alloy shows the Gaussian unitary ensemble (GUE) statistics. However, for both the Si crystal and the $Al_xGa_{1-x}As$ alloy the spectral statistics of the band structures around a symmetric point in the BZ show deviations from their corresponding Gaussian ensemble statistics. In particular, it is shown that for a small value of the fraction x, the $Al_xGa_{1-x}As$ band structure at the Γ point shows Poisson-like statistics. The spectral statistics were also analysed for the magnetic band structures of two-dimensional (2D) as well as one-dimensional (1D) surface periodic systems (i.e., surface superlattices) in perpendicularly applied magnetic fields. For the 2D surface superlattices [15], the statistics of the magnetic band structure is found to show similar properties to the three-dimensional (3D) Si crystal and $Al_xGa_{1-x}As$ alloy: at a sufficiently strong magnetic field, the magnetic band structure of a 2D surface superlattice at the magnetic wave vector away from any point of symmetry in the magnetic BZ (MBZ) can be well described by the GUE statistics, while the magnetic band structure along symmetric lines in the MBZ can be well described by GOE statistics and the magnetic band structure at the points of higher symmetry (Γ, A, and M) shows Poisson-like statistics. For a 1D surface superlattice with inversion symmetry [16, 17], it was found that for the wave vector k not in the close vicinity of a symmetric point (e.g., the $k = 0$ point) the magnetic band structure shows the GOE statistics. It was also found that the band structure of the 1D surface superlattice deviates from the GOE statistics when the wave vector k is moved towards a symmetric point. However, the spectral statistics has not been analysed for the system exactly at a symmetric k-point.

In this work, we make a detailed study of the spectral statistics for 1D surface superlattices in perpendicularly applied magnetic fields at the $k = 0$ point. An interesting result found in this study is that the spectra of the systems at this point show the statistics derived by a superposition of two independent GOE statistics. By contrast, we note that the results found in references [14, 15] indicate that the spectra of the 2D surface superlattices in magnetic fields and of the 3D $Al_xGa_{1-x}As$ ($x < 0.1$) system at the corresponding highly symmetric points in the MBZ or BZ show Poisson-like statistics. The paper is organized as follows. In section 2, we describe the model and its symmetric properties. Also in this section we briefly describe the theoretical framework of quantum chaos used in this study. In section 3, we present our numerical results and discuss them in terms of the symmetry of the system. Finally, section 4 contains a summary and conclusions.

2. Model and theory

The 1D periodic system considered in this work is a square, antidot (repulsive potential) lattice implanted in the $x - y$ plane with a period a in a wide channel of width w. The potential of the antidot lattice was assumed to be

$$V(x, y) = \begin{cases} V_0\{\cos[\pi x/a]\cos[\pi(y - y_0)/a]\}^{2\beta} & \text{if } |y| \leqslant w/2 \\ \infty & \text{if } |y| > w/2 \end{cases} \tag{1}$$

where $|x| < \infty$, V_0 and integer β control the strength and steepness of the antidot potential, while $|y_0| \leqslant a/2$ controls the peak positions of the antidot potential along the transverse y-direction. In the present work, the assumption that $V_0 = 1$ eV and $\beta = 10$ was made. The lattice spacing was taken to be $a = 100$ nm and the channel width $w = 400$ nm, so the antidot potential has four periods along the transverse y-direction.

The motion of a spinless electron in the system in the magnetic field $\vec{B} = (0, 0, B)$ is described by the Hamiltonian

$$H = \frac{1}{2m^*}[\vec{P} + e\vec{A}(x, y)]^2 + V(x, y) \tag{2}$$

where m^* is the effective mass of the electron and $\vec{A} = (-By, 0, 0)$ is the vector potential in the Landau gauge. The assumption of $m^* = 0.067m_e$, appropriate for an $Al_xGa_{1-x}As/GaAs$ system, was made when the numerical calculations for this work were performed.

The translation invariance of the Hamiltonian allows us to reduce the quantum-mechanical problem to the study of the electron motion in a single unit cell. Using Bloch's theorem, the Schrödinger equation can be written as

$$H_k u_k(x, y) = E(k)u_k(x, y) \tag{3}$$

where k is the Bloch wave vector in the x-direction, $u_k(x + a, y) = u_k(x, y)$ is the periodic part of the electron wave function, and the reduced Hamiltonian H_k is

$$H_k = -\frac{\hbar^2}{2m^*}\left(\frac{\partial^2}{\partial x^2} + \frac{\partial^2}{\partial y^2}\right) - \frac{i\hbar^2}{m^*}\left(k - \frac{eBy}{\hbar}\right)\frac{\partial}{\partial x} + \frac{\hbar^2}{2m^*}\left(k - \frac{eBy}{\hbar}\right)^2 + V(x, y). \tag{4}$$

Equation (3) with the Hamiltonian given in equation (4) was solved numerically for a given wave vector k and magnetic field B using the method described in reference [16]. The conventional band structure of the system can be obtained by plotting the eigenvalues $E_n(k, B)$ (with n being the band index) as a function of the wave vector k for a given value of B, while the magnetic band structure of the system is obtained by presenting the calculated eigenvalues $E_n(k, B)$ as a function of B at a given k.

The Hamiltonian H_k presented in equation (4) has certain symmetries. The spectral statistical properties are closely related to the symmetries of the system. Knowing these symmetries is, therefore, very necessary for understanding the results presented in the next section. Below, we describe symmetric properties of the system in some selected cases.

(a) The case of $k = 0$, $B = 0$, and $y_0 = 0$: the Hamiltonian H_k is, geometrically, highly symmetric in this case. It has the symmetry of inversion I (i.e., $(x, y) \to (-x, -y)$) and the symmetries of reflections R_x (i.e., $x \to -x$) and R_y (i.e., $y \to -y$). Solutions to the Schrödinger equation (3) can therefore be divided into four different classes according to whether or not they are even or odd under R_x and R_y. In addition, H_k is also invariant under the time-reversal (T) operation.

(b) The case of $k = 0$, $B = 0$, and $y_0 \neq 0$ or $\pm a/2$: the geometrical symmetry is reduced in this case and H_k is geometrically symmetric only under R_x. H_k is still invariant under T.

(c) The case of $k = 0$, $B \neq 0$, and $y_0 = 0$: H_k is geometrically symmetric only under I in this case. In addition, a finite value of B breaks the T-symmetry in H_k. However, the Hamiltonian H_k is invariant under anti-unitary operation of TR_x or TR_y; that is, it shows *false* T-violation.

(d) The case of $k = 0$, $B \neq 0$, and $y_0 \neq 0$ or $\pm a/2$: the Hamiltonian H_k is invariant only under anti-unitary operation of TR_x.

(e) The case of $k \neq 0$ or $\pm\pi/a$, $B = 0$, and $y_0 = 0$: H_k is geometrically symmetric only under R_y and has no T-symmetry. However, it is still invariant under TR_x.

(f) The case of $k \neq 0$ or $\pm\pi/a$, $B \neq 0$, and $y_0 = 0$: the only symmetry seen in this case is that H_k is invariant under TR_x.

The spectral statistics for the system in some of these cases listed above have been studied previously [16]. In the present work, we shall only study the spectral statistics for the system in the cases of (c), (d), and (f). Among the three cases, only in case (c) has H_k got a geometrical

symmetry—namely, it is invariant under the operation of inversion I. However, in all three cases, H_k is invariant under anti-unitary operation of TR_x, i.e., it shows a *false* T-violation. We shall make a comparison between the spectral statistics obtained for the three cases and discuss their common features and differences in terms of the symmetries of H_k.

The two most frequently studied characteristics of spectral statistics are the level-spacing distribution $P(s)$, where s is the nearest-neighbour level spacing (hereafter we will always express the energy in units of mean level spacing), and the Dyson–Mehta statistic Δ_3. $P(s)$ measures the level repulsion; it is normalized. Δ_3 measures the rigidity of the spectrum; it is given by the variance of the number of energy eigenvalues found in an energy interval of length L:

$$\Delta_3(L) = \frac{1}{L}\left\langle \min_{a,b} \int_{\bar{E}-L/2}^{\bar{E}+L/2} \mathrm{d}E\ [N(E) - aE - b]^2 \right\rangle \tag{5}$$

where $N(E)$ is the number of energy levels below the energy E and the angle brackets indicate the statistical average. It is well known that in terms of random-matrix theory (RMT), both $P(s)$ and Δ_3 can be approached using analytical expressions (see, for example, reference [18] for a detailed discussion of the approach and reference [16] for the details of the expressions for various ensembles).

It should be emphasized again that at $k = 0$ or $\pm\pi/a$, the Hamiltonian H_k in equation (4) with $y_0 = 0$ (cf. equation (1)) is invariant under the inversion I (i.e., $(x, y) \to (-x, -y)$) and the energy levels can be degenerate. Theoretically, we can always group these energy levels into two sets according to the parity of their wave functions with respect to the inversion. This procedure corresponds to transforming the Hamiltonian matrix H_k into a two-block diagonal matrix. Each block corresponds to a submatrix which, when diagonalized, gives one set of energy levels, and the two submatrices are mutually independent, but still show the false T-violation, like the original Hamiltonian H_k. However, in experiment it is often the case that the two sets of energy levels cannot be separately measured. One would then like to know what the statistical properties of the combined system are.

Following the arguments given by Gurevich and Pevsner [19], it can be shown that the level-spacing distribution, $P_{2\mathrm{GOE}}(s)$, of the system resulting from the combination of two mutually independent sequences with the GOE level-spacing distribution, $P_{\mathrm{GOE}}(s)$, can be approached by using

$$P_{2\mathrm{GOE}}(s) = 2\frac{\mathrm{d}}{\mathrm{d}s}\left[\Psi_{\mathrm{GOE}}(s)\frac{\mathrm{d}}{\mathrm{d}s}\Psi_{\mathrm{GOE}}(s)\right] \tag{6}$$

where

$$\Psi_{\mathrm{GOE}}(s) = \frac{1}{2}\int_{s/2}^{\infty}(2t - s)P_{\mathrm{GOE}}(t)\,\mathrm{d}t. \tag{7}$$

Inserting the expression for $P_{\mathrm{GOE}}(s)$ into the above equation gives an analytical expression for the level-spacing distribution of the combined system:

$$P_{2\mathrm{GOE}}(s) = \frac{1}{2}\exp\left(-\frac{\pi}{8}s^2\right) + \frac{\pi}{8}s\exp\left(-\frac{\pi}{16}s^2\right)\left[1 - \int_0^{s/2}\exp\left(-\frac{\pi}{4}t^2\right)\mathrm{d}t\right]. \tag{8}$$

It is easy to verify that $P_{2\mathrm{GOE}}(0) = 1/2$ and $\mathrm{d}P_{2\mathrm{GOE}}(0)/\mathrm{d}s = (1/4)\ \mathrm{d}P_{\mathrm{GOE}}(0)/\mathrm{d}s = \pi/8$. Since the Dyson–Mehta statistic Δ_3 is a quadratic functional of the level density, its value for the combined system, $\Delta_{3,2\mathrm{GOE}}(L)$, is simply additive for the two mutually independent spectral sequences with the GOE statistics $\Delta_{3,\mathrm{GOE}}$. Thus

$$\Delta_{3,2\mathrm{GOE}}(L) = 2\Delta_{3,\mathrm{GOE}}(L/2). \tag{9}$$

From now on, we will call the statistics derived by a superposition of two independent GOE statistics the double-GOE statistics. An analytical expression for the double-GUE statistics, derived from a superposition of two independent GUE statistics, can be found in reference [20].

3. Numerical results and discussion

The numerical calculations of these statistical characteristics for the surface superlattice considered in this work were carried out as follows. We first generated magnetic band structures for the system at various given k-values. In each magnetic band structure, the energy eigenvalues for a finite number of magnetic field values were taken. The spectra were then unfolded using a standard procedure described in reference [21] (see also reference [16]). The statistical average was taken over different values of the magnetic field and over a large number of energy bands.

Before we present our numerical results, we would like to note that when evaluating the spectral statistics the average needs to be taken over an appropriate range of magnetic field values. As we discussed above, the Hamiltonian H_k at $B = 0$ can have more symmetries than the Hamiltonian at $B \neq 0$ (cf. equation (4)). Thus, in the calculation of the spectral statistics for the magnetic band structure at $B \neq 0$, we need to take the statistical average over the calculations at the magnetic fields that are strong enough to suppress the traces of the extra symmetries in the spectra. We have found numerically that a magnetic field of $B = 0.2$ T is sufficient for the suppression. However, we should also avoid the statistical average over the calculations at very high magnetic fields. This is because electrons tend to be localized at high magnetic field and do not 'see' very well the precise profile of the antidot potential when the magnetic field becomes higher than a critical value B_c. Semiclassically, the critical field B_c can be approximately determined by setting the cyclotron radius ℓ_c of the electrons equal to the lattice constant a. Note that B_c depends on the energy of the electrons and increases with increase of the energy. Note also that good statistics require that ℓ_c be sufficiently larger than the lattice constant a. In the present work, we have excluded the eigenvalues in the lowest 200 magnetic bands and have calculated the spectral statistics by taking the average over the magnetic band energies evaluated for the magnetic field values in the range 0.3–1.2 T. Our results of the calculations are presented in figure 1 to figure 6.

Figure 1 shows a portion of the magnetic band structure calculated for $k = 0$ and $y_0 = 0$. It can be clearly seen that the spectral complexity is well developed in the magnetic band structure, except that there is clear evidence of level degeneracy in the sense that some lines tend to pair up together and move side by side as the magnetic field increases. This degeneracy effect correctly reflects the symmetry of the Hamiltonian H_k under inversion I in the case of $k = 0$, $B \neq 0$, and $y_0 = 0$. Figure 2 shows our numerical results on the spectral statistics extracted from a set of the energy eigenvalues of the magnetic band structure at $k = 0$ and $y_0 = 0$ with band index $n = 200$ to 600 (corresponding to an energy range in about 40 to 120 meV) computed for 91 equally spaced magnetic field values in the range 0.3 to 1.2 T. It is clear that the spectral statistics deviates strongly from the GOE and GUE distributions in this case. However, equations (8) and (9) provide an excellent description for the statistics of the energy spectra. This result is consistent with the fact that the Hamiltonian H_k in this case shows a false T-violation and the geometrical symmetry under I. The false T-violation suffices to lead the spectra to the GOE statistics [20], while the combination of the false T-violation and the inversion symmetry should lead the spectra to the double-GOE statistics (see the discussion leading to equations (8) and (9)).

At this point, we would like to note that the spectral statistics have also been analysed for the band structures of a 3D $Al_xGa_{1-x}As$ alloy and a 2D surface superlattice at the symmetrical

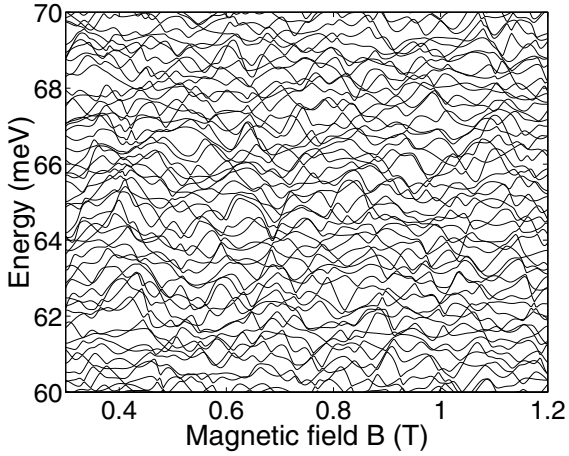

Figure 1. A portion of the magnetic band structure of the Q1D surface superlattice at $k = 0$ and $y_0 = 0$.

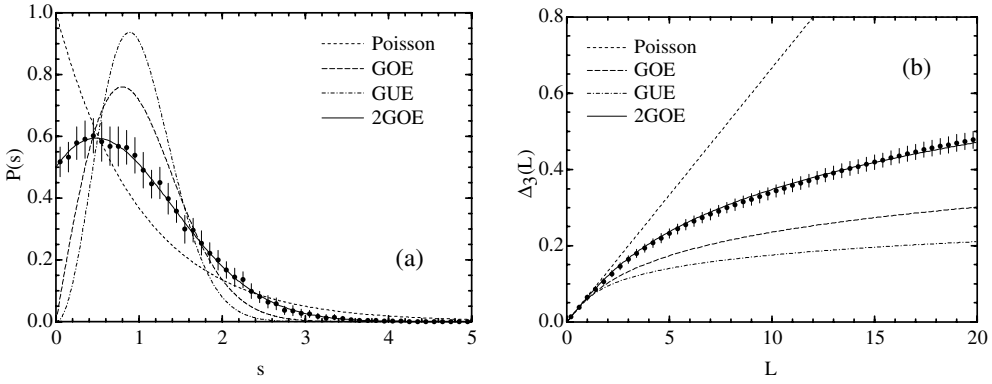

Figure 2. The spectral statistics for the magnetic band structure of the Q1D surface superlattice as shown in figure 1 for the case of $k = 0$ and $y_0 = 0$. The data (indicated by solid dots with error bars) were extracted from the energy eigenvalues of 401 energy bands with the band index $n = 200$ to 600 and 91 equally spaced magnetic field values in the range $B = 0.3$ to 1.2 T. (a) shows the band-spacing distribution $P(s)$; (b) shows the Dyson–Mehta statistic $\Delta_3(L)$. The short-dashed, long-dashed, and dash–dotted curves give the theoretical predictions for the Poisson, GOE, and GUE statistics, respectively. The solid curves show the predictions for the system obtained from the superposition of two mutually independent sequences with the GOE statistics (equations (8) and (9)).

point $\vec{k} = 0$ in the BZ or MBZ [14, 15]. These analyses indicate that the spectra of the two periodic systems at the symmetrical point $\vec{k} = 0$ tend to show Poisson-like statistics (note that for the 2D surface superlattice the $\Delta_3(L)$ statistic even shows a logarithmic increase [15]). Clearly, the result of our analysis on the spectral statistics for the 1D surface superlattice at the symmetric point $k = 0$ is different from these early analyses. We should, however, emphasize that our result is consistent with the fact that the Hamiltonian H_k in the case considered shows a false T-violation and the inversion symmetry.

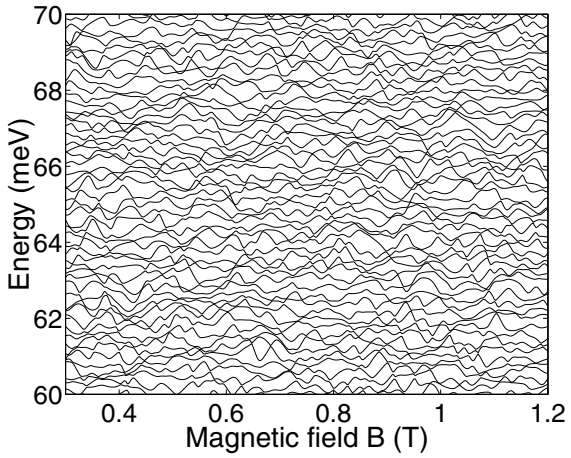

Figure 3. A portion of the magnetic band structure of the Q1D surface superlattice at $k = 0.5\,\pi/a$ and $y_0 = 0$.

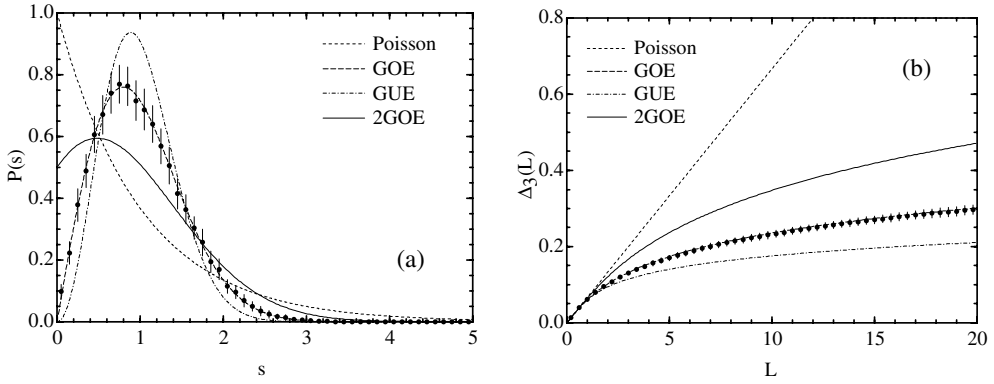

Figure 4. Spectral statistics for the magnetic band structure of the Q1D surface superlattice as shown in figure 3 for the case of $k = 0.5\,\pi/a$ and $y_0 = 0$. The data (indicated by solid dots with error bars) were extracted from the energy eigenvalues of 401 energy bands with the band index $n = 200$ to 600 and 91 equally spaced magnetic field values in the range $B = 0.3$ to 1.2 T. (a) shows the band-spacing distribution $P(s)$; (b) shows the Dyson–Mehta statistic $\Delta_3(L)$. The short-dashed, long-dashed, and dash–dotted curves give the theoretical predictions for the Poisson, GOE, and GUE statistics, respectively. The solid curves show the predictions for the system obtained from the superposition of two mutually independent sequences with the GOE statistics.

When we break the inversion symmetry, we should remove the degeneracy from the energy spectra of our 1D periodic systems and expect to observe that the spectra move from the double-GOE to the GOE statistics. The symmetry breaking can be realized in our system either by making the wave vector k finite, but not equal to $\pm\pi/a$ (i.e., case (f) in the previous section) or by shifting y_0 away from zero and from multiples of $a/2$ (i.e., case (d) in the previous section). Figure 3 shows a portion of the magnetic band structure calculated for $k = 0.5\pi/a$ and $y_0 = 0$. When comparing this figure with figure 1, one seems to see that the levels cover the energy space more densely in this case than in that of figure 1. In fact, this is not the case. The energy spectra in the two cases have approximately equal averaged level

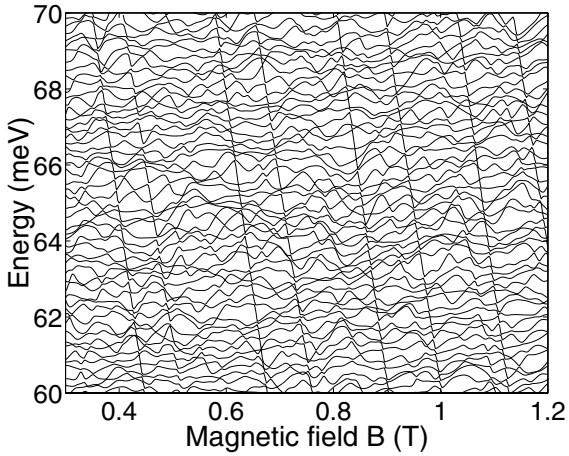

Figure 5. A portion of the magnetic band structure of the Q1D surface superlattice at $k = 0$ and $y_0 = 0.25\,a$ (25 nm).

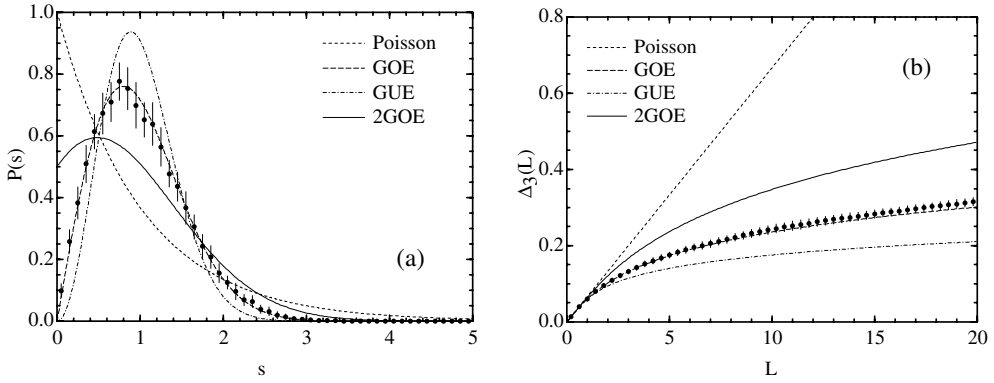

Figure 6. Spectral statistics for the magnetic band structure of the Q1D surface superlattice as shown in figure 5 for the case of $k = 0$ and $y_0 = 0.25\,a$. The data (indicated by solid dots with error bars) were extracted from the energy eigenvalues of 401 energy bands with the band index $n = 200$ to 600 and 91 equally spaced magnetic field values in the range $B = 0.3$ to 1.2 T. (a) shows the band-spacing distribution $P(s)$; (b) shows the Dyson–Mehta statistic $\Delta_3(L)$. The short-dashed, long-dashed, and dash–dotted curves give the theoretical predictions for the Poisson, GOE, and GUE statistics, respectively. The solid curves show the predictions for the system obtained from the superposition of two mutually independent sequences with the GOE statistics.

densities in the energy range that we considered. This is because possible level degeneracy exists in the case considered in figure 1. Figure 4 shows the numerical results on the spectral statistics extracted from a set of the energy eigenvalues in the magnetic energy bands with band index $n = 200$ to 600 (corresponding to an energy range in about 40 to 120 meV) computed for 91 magnetic field values (equally spaced in the range 0.3 to 1.2 T) at $k = 0.5\pi/a$ and $y_0 = 0$. Notice that a good agreement with the GOE statistics is found, as we expected.

Figure 5 shows a portion of the magnetic band structure calculated for $k = 0$ and $y_0 = a/4$. Here, an averaged level density similar to that in figure 3 is seen and the spectra show no degeneracy. However, some clean, parallel features are clearly visible in the calculated

magnetic band structure shown in figure 5. We expect that these clean features should have effects on the spectral statistics. Figure 6 shows the numerical results on the spectral statistics extracted from a set of the energy eigenvalues in the magnetic energy bands with band index $n = 200$ to 600 (corresponding to an energy range of about 40 to 120 meV) computed for 91 magnetic field values (equally spaced in the range 0.3 to 1.2 T) at $k = 0$ and $y_0 = a/4$. Although for $P(s)$ a good GOE statistic is found here, for $\Delta_3(L)$ deviation from the GOE prediction is clearly visible at large L. The deviation appears as a result of existing clean features in the spectra (see figure 5).

4. Summary and conclusions

We have studied symmetry and spectral properties of a quasi-one-dimensional superlattice in perpendicularly applied magnetic fields. Two statistical characteristics, namely, the energy-level-spacing distribution and the Dyson–Mehta Δ_3 statistic, of the energy band structure of the system have been calculated. Time-reversal (T-) symmetry is broken in the system. However, the system is invariant under the anti-unitary combination of symmetric operations which includes T, leading to what is called *false* T-violation. For the wave vector k not in the close vicinity of a symmetrical point in k-space, the statistical properties of the magnetic band structure are found to be described by the statistics of the GOE. This result is in agreement with the prediction that the false T-violation suffices to give the energy spectra the properties of the GOE, instead of those of the GUE. However, the magnetic band structure is found to deviate from the GOE statistics at $k = 0$, if the system is invariant under the inversion. We have shown that the magnetic band structure in this case is well described by the double-GOE statistics, derived for systems that possess two mutually independent sets of energy levels of the same density with the GOE statistics.

Acknowledgments

This work was supported by the Swedish Research Council for Engineering Sciences (VR/TFR) and the Swedish Foundation for Strategic Research (SSF). One of us (HQX) gratefully acknowledges the support of K C Wong Education Foundation, Hong Kong.

References

[1] Haake F 1992 *Quantum Signatures of Chaos* (Berlin: Springer)
[2] Camarda H S and Georgopulos P D 1983 *Phys. Rev. Lett.* **50** 492
[3] Wintgen D, Holle A, Wiebusch G, Main J, Friedrich H and Welge K H 1986 *J. Phy. B: At. Mol. Phys.* **19** L557
[4] Karremans K, Vassen W and Hogervorst W 1998 *Phys. Rev. Lett.* **81** 4843
[5] Haq R U, Pandey A and Bohigas O 1982 *Phys. Rev. Lett.* **48** 1086
[6] Bohigas O, Haq R U and Pandey A 1985 *Phys. Rev. Lett.* **54** 1645
[7] Bohigas O, Giannoni M J and Schmit C 1984 *Phys. Rev. Lett.* **52** 1
[8] Ji Z-L and Berggren K-F 1995 *Phys. Rev. B* **52** 1745
[9] Ellegaard C, Guhr T, Lindemann K, Lorensen H Q, Nygård J and Oxborrow M 1995 *Phys. Rev. Lett.* **75** 1546
[10] Bertelsen P, Ellegaard C and Hugues E 2000 *Eur. Phys. J.* B **15** 87
[11] Stöckmann H-J and Stein J 1990 *Phys. Rev. Lett.* **64** 2215
[12] Gräf H-D, Harney H L, Lengeler H, Lewenkopf C H, Rangacharyulu C, Richter A, Schardt P and Weidenmüller H A 1992 *Phys. Rev. Lett.* **69** 1296
[13] Miyazaki S and Kolovsky A R 1994 *Phys. Rev.* E **50** 910
[14] Mucciolo E R, Capaz R B, Altshuler B L and Joannopoulos J D 1994 *Phys. Rev.* B **50** 8245
[15] Silberbauer H, Rotter P, Rössler U and Suhrke M 1995 *Europhys. Lett.* **31** 393
[16] Xu H Q 1998 *J. Phys.: Condens. Matter* **10** 4001

[17] Xu H Q 1996 *Proc. 23rd Int. Conf. on the Physics of Semiconductors* ed M Scheffler and R Zimmermann (Singapore: World Scientific) p 1489
[18] Mehta M L 1991 *Random Matrices* (New York: Academic)
[19] Gurevich I I and Pevsner M I 1956/7 *Nucl. Phys.* **2** 575
[20] Robnik M and Berry M V 1986 *J. Phys. A: Math. Gen.* **19** 669
[21] Bohigas O and Giannoni M J 1975 *Ann. Phys.* NY **89** 393